Study on Reactor Building Structure Using Ultrahigh Strength Materials Part 4 Bending Shear Tests of RC Shear Walls

Toshiaki UCHIYAMA
Shimizu Coporation, Tokyo, Japan
Kikuo ISHIMURA
Tokyo Electric Power Company, Tokyo, Japan
Toshio TAKAHASHI
Kajima Corporation, Tokyo, Japan
Tohru HIRADE
Takenaka Corporation, Tokyo, Japan

ABSTRACT

This paper describes the structural characteristics of reinforced concrete shear wall using ultrahigh strength materials such as concrete of 98.1MPa comressive strength and rebars of 785MPa yeild strength under bending shear stresses.

1 INTRODUCTION

The purpose of the present study is to study the possibility of applying ultrahigh strength concrete and steel bars (abbr.rebars) to nuclear reactor buildings effectively by investigating experimentally the structural characteristics of reinforced concrete (abbr.RC) shear walls which are H-shaped with flange under bending shear stresses.
At first the experimental procedure and the outline of results are described. Then the effects of the parameters such as concrete compressive strength, rebar yield strength, reinforcement quantity (product of rebar ratio and yield strength) on the structural characteristics of the shear walls are studied. Further, the applicability of proposed formulae to the shear walls using ultrahigh-strength materials are investigated by the comparison of the experimental results with the results calculated by the formulae.

2 EXPERIMENTAL PROCEDURE

The detail of specimens is shown in Fig.1. The shear span ratio M/QD is 0.8 and both of web and flange are 12cm in thickness. The nine specimens as shown in Table 1 are chosen which are made by the combination of the following parameters: concrete compressive strength Fc (39,69,98MPa [400,700,1000 kgf/cm^2]), rebar yield strength $s\sigma y$ (392,588,785MPa [4000, 6000,8000kgf/cm^2]) and reinforcement quantity $P_s \cdot s\sigma_y$ (product of rebar ratio P_s and yield strength $s\sigma y$ (4.7,6.3,7.1 MPa [48,72,96kgf/cm^2]).
The cyclic lateral loading is applied at the top of specimens under a constant axial stress σ_0=1.96MPa as shown in Fig.2. The loading cycles are shown in Fig.3.

3 EXPERIMENTAL RESULTS

3.1 OUTLINE OF RESULTS

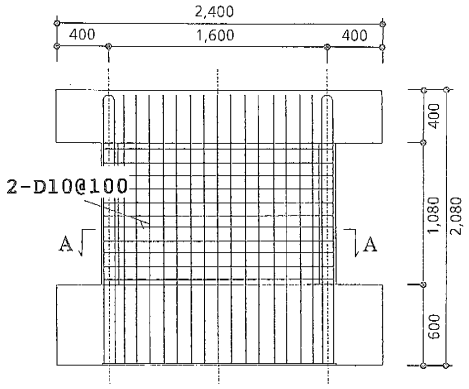

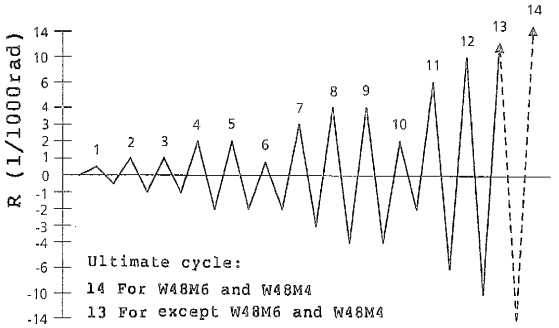

Fig.3 Lateral loading cycles

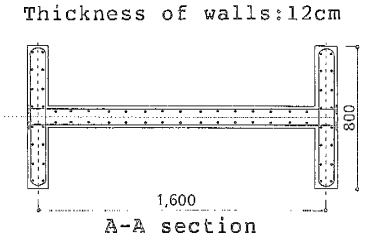

Fig.1 Detail of specimens (Ps=1.2%)

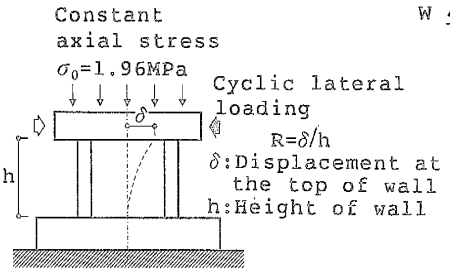

Fig.2 Loading to specimens

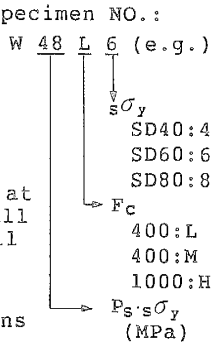

Table 1 Properties of specimens and principal results

SPECIMENS		W48L6	W48M6	W48L4	W48M4	W72L6	W72M8	W72M6	W72H8	W96H8
Concrete compressive strength F_c (MPa)		48.5 (39.2)	82.4 (68.6)	48.5 (39.2)	82.4 (68.6)	48.5 (39.2)	82.4 (68.6)	82.4 (68.6)	101.9 (98.1)	101.9 (98.1)
Reinforcement quantity $_sP_s \cdot \sigma_y$ (MPa)		4.42 (4.71)	4.42 (4.71)	4.10 (4.71)	4.10 (4.71)	6.61 (7.06)	7.21 (7.06)	6.61 (7.06)	7.21 (7.06)	9.35 (9.41)
Rebar yield strength $_s\sigma_y$ (MPa)		560 (SD60)	560 (SD60)	347 (SD40)	347 (SD40)	560 (SD60)	792 (SD80)	560 (SD60)	792 (SD80)	792 (SD80)
Concrete Young's modulus E_c ($\times 10^4$MPa)		3.14	3.94	3.14	3.94	3.14	3.94	3.94	3.81	3.81
Concrete Poisson's ratio ν		0.19	0.21	0.19	0.21	0.19	0.21	0.21	0.21	0.21
Rebar Young's modulus E_s ($\times 10^5$MPa)		1.95	1.95	1.99	1.99	1.95	1.93	1.95	1.93	1.93
Reinforcement ratio P_s (%)	Web	0.79 (0.8)	0.79 (0.8)	1.18 (1.2)	1.18 (1.2)	1.18 (1.2)	0.91 (0.9)	1.18 (1.2)	0.91 (0.9)	1.18 (1.2)
	Flange	0.89 (0.8)	0.89 (0.8)	1.19 (1.2)	1.19 (1.2)	1.19 (1.2)	0.89 (0.9)	1.19 (1.2)	0.89 (0.9)	1.19 (1.2)
Shear cracking stress τ_{cr} (MPa)		4.25	4.49	3.63	3.27	4.19	2.92	3.05	4.09	3.95
Shear stress at the yielding of flange rebars τ_y (MPa)		6.92	6.51	6.09	63.2	7.93	8.75	8.31	9.65	10.39
Deflection angle at the yielding of flange rebars R (1/1000)		4.68	3.15	2.81	2.44	4.46	5.39	4.01	5.79	6.39
Maximum shear strength τ_u (MPa)		7.72	7.90	7.16	7.71	10.01	10.77	10.50	11.09	12.94
Defection angle at maximum shear strength R_u (1/1000)		9.05	6.01	6.09	10.05	10.26	10.14	10.23	10.05	10.22
Equivalent viscous damping factor h_e (%) at R=1/3000 (Shear deformation γ=2/1000)		6.49	6.39	6.03	6.30	8.30	8.34	6.13	7.26	6.27
Failure mode		Sliding shear	Compr-ession	Compr-ession	Compr-ession	Sliding shear	Breaking of rebars	Sliding shear	Breaking of rebars	Breaking of rebars

( ):Planning value

① Cracking at the corner of web
② Flexural cracking at the bottom of flange
③ Diagonal cracking in web
④ Flexural cracking except at the bottom of flange
⑤ Yielding of vertical rebars in flange
⑥ Yielding of vertical rebars in web
⑦ Compressive failure at the corner of web
⑧ Yielding of horizontal rebars in web
⑨ Sliding shear failure
⑩ Breaking of vertical rebars in flange

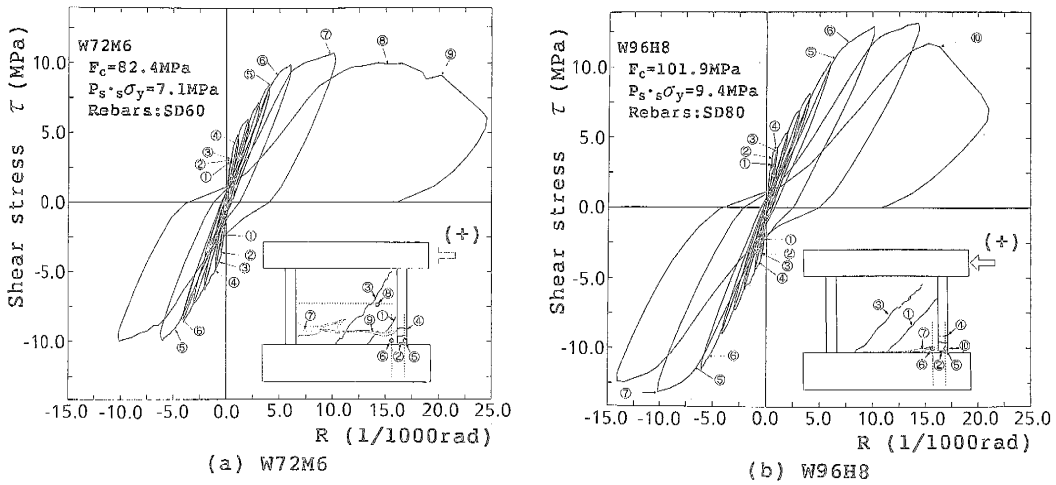

(a) W72M6 (b) W96H8

Fig.4 Shear stress-deflection angle relationship and test progress

The principal results are given in Table 1 such as the shear cracking stress τ_{cr}, the shear stress τ_y and the deflection angle R_y at the yielding of the vertical rebars in the flange, the maximum strength τ_u, the deflection angle R_u at maximum strength, the equivalent viscous damping factors h_e of load-shear deformation γ relationship and the failure modes.
The values of τ_{cr}, which are the shear stresses when the first diagonal cracks appear in the web, are approximately within the range from 3MPa to 4.5MPa.
The maximum shear stress τu of every specimen is larger than the result of $P_s \cdot s\sigma_y + \sigma_0$. It indicates that the reinforcement is effective on the strength of shear walls also using ultrahigh strength materials. The specimens which $P_s \cdot s\sigma_y$ are 7.1MPa and 9.4MPa reach the maximum strength when the deflection angle R is about 10/1000rad.
The equivalent viscous damping factors h_e of all specimens are larger than 6% when γ at the peak of the hysteresis loop is almost 2/1000rad (R=3/1000rad), established as the allowable limit of the shear deformation for the design of nuclear reactor buildings (J.Kodama, 1987).
The failure modes are the sliding shear failure for three specimens, the compression failure for three specimens and the breaking of the rebars at the bottom of the flange for three specimens.
The shear stress-deflection angle relationship and the test progress of W72M6 and W96H8 are shown in Fig.4. The progresses of all specimens are almost same as these specimens except ultimate failure. The slipping of the hysteresis loops occurred in case of all specimens as deflection increased.

3.2 PARAMETRIC STUDY

The relationship between the shear cracking stress τ_{cr} and the concrete compressive strength Fc is shown in Fig.5. The stress τ_{cr} does not increase much as Fc rise from 48.5MPa to 101.9 MPa. The relationship between the maximum shear stress τ_u and Fc is shown in Fig.6. The stress τ_u increases slightly as Fc increases.

The relationship between the deflection angle R_u at maximum strength and the reinforcement quantity $P_s \cdot {}_s\sigma_y$ is shown in Fig.7. The angle R_u increases as $P_s \cdot {}_s\sigma_y$ rise from 4.7MPa to 7.1MPa, while R_u at $P_s \cdot {}_s\sigma_y$=9.4MPa is same as at $P_s \cdot {}_s\sigma_y$=7.1MPa. The relationship between the maximum shear stress τ_u and $P_s \cdot {}_s\sigma_y$ is shown in Fig.8. The stress τ_u is influenced by $P_s \cdot {}_s\sigma_y$ considerably and the relation between τ_u and $P_s \cdot {}_s\sigma_y$ is nearly linear

The relationship between the maximum shear stress τu and the rebar yield strength ${}_s\sigma_y$ is shown in Fig.9. τ_u increases slightly as ${}_s\sigma_y$ rise, so the effect of ${}_s\sigma_y$ on τ_u is not significant. The relationship between the equivalent viscous damping factor h_e and the deflection angle at the peaks of cycles for W48L4 and W48L6 is shown in Fig.10 which specimens are deferent only in rebar yield strength ${}_s\sigma_y$. The factor h_e of the specimens which ${}_s\sigma_y$ is higher are less than that which ${}_s\sigma_y$ is lower as deflection increases.

4 APPLICABILITY OF PROPOSED FORMULAE

The comparison of the experimental results of maximum shear strength τ_u with

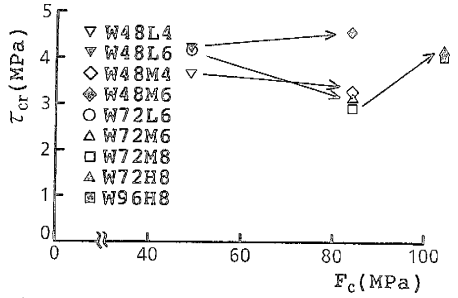

Fig.5 Shear cracking stress-concrete compressive strength relationship

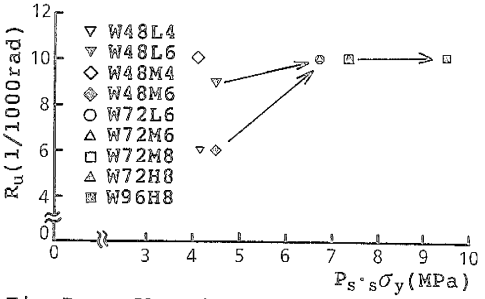

Fig.7 Deflection angle at maximum strength-reinforcement quantity relationship

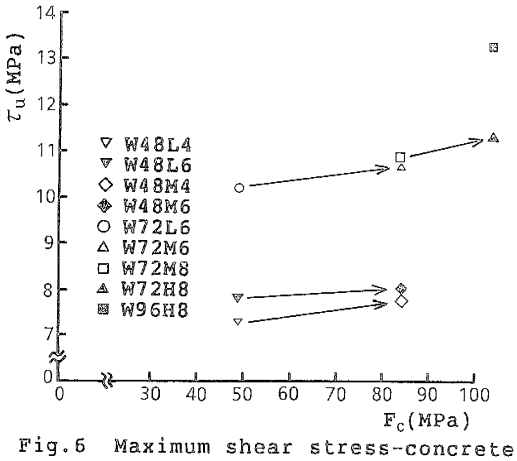

Fig.6 Maximum shear stress-concrete compressive strength relationship

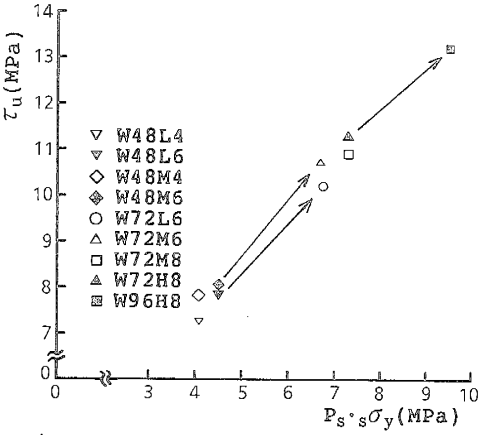

Fig.8 Maximum shear stress-reinforcement quantity relationship

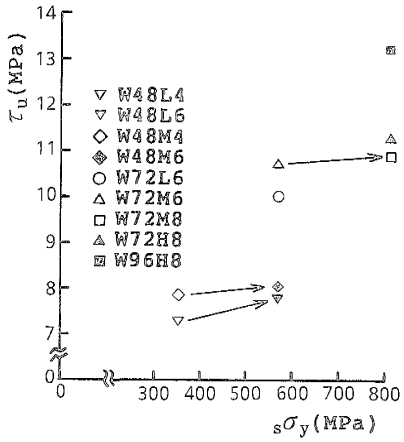

Fig.9 Maximum shear stress-rebar yield strength relationship

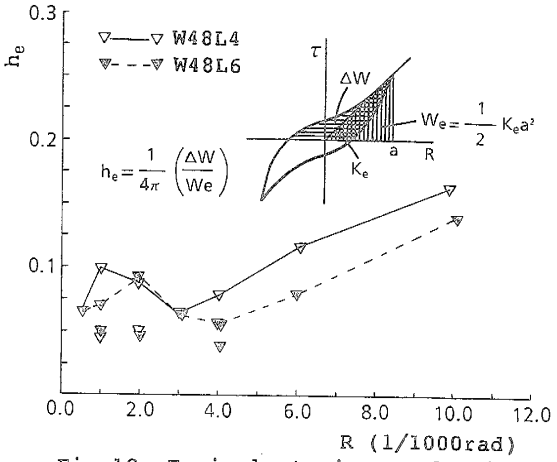

Fig.10 Equivalent viscous damping factor-deflection angle relationship

the results calculated by three proposed formulae; (1)(S.Inoue and N.Suzuki, 1989), (2)(K.Shiraishi and Y.Kanoh, 1989) and (3) (S.Furukawa et al, 1987) are shown in Fig.11. The experimental results agree well with the results calculated by the three formulae, which properly reflect the differences in concrete compressive strength, reinforcement quantity and rebar yield strength. The values of maximum shear stress can be properly predicted by their equations.

The comparison of the experimental results of shear stress-deflection angle relationship with the results calculated by the three formulae are shown in Fig.12 respectively. The results by the formula (1) agree with the experimental results within the range from yielding of vertical rebars in the flange to maximum strength for all specimens. The results by the formula (2) agree well with the experimental results except in the range near maximum strength for the specimens using ultrahigh strength materials such as W96H8. In case of the formula (3) the agreement in the specimens with lower concrete compressive strength Fc is better than in the specimens with higher Fc.

From these results it is found that the relations between shear stress and deflection of the specimens also using ultrahigh strength materials can be approximately predicted by the proposed formulae.

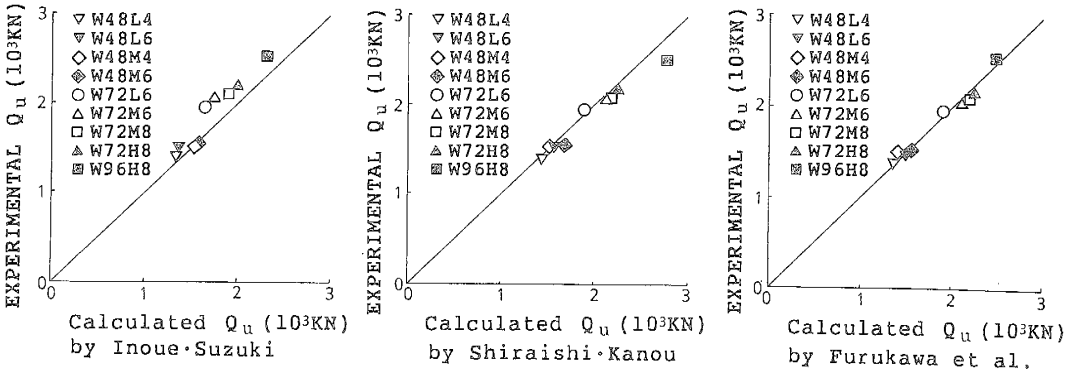

Fig.11 Comparison of experimental results of maximum shear strength with calculated results

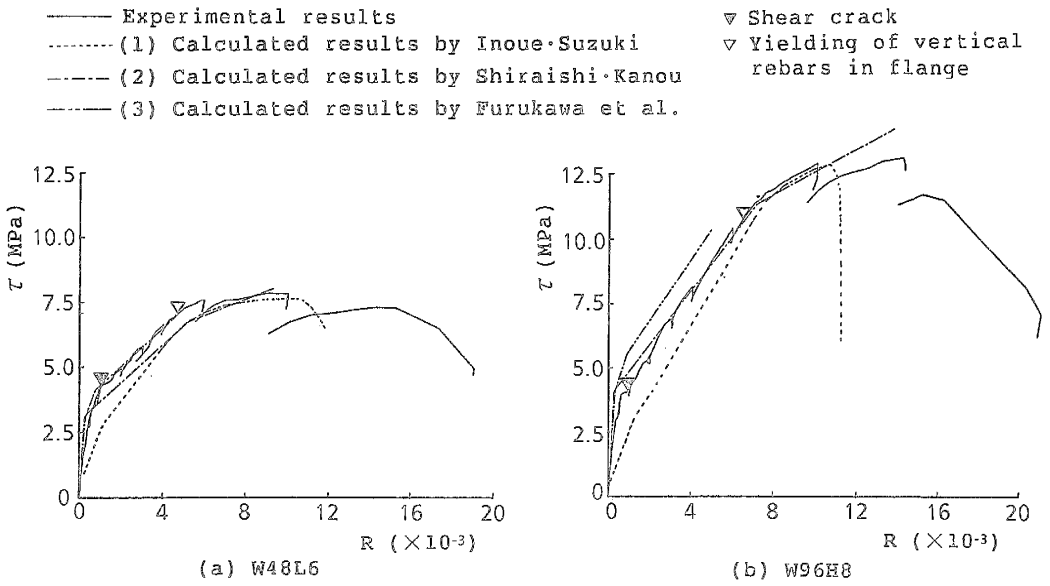

Fig.12 Comparison of experimental results with calculated results of shear stress- deflection angle relationship

5 CONCLUSION

The structural characteristics of the shear walls of using ultrahigh strength materials were grasped, and the experimental results were compared with the results calculated by the proposed formulae.
As a result, it was found that the characteristics of the RC shear wall using ultrahigh strength materials can be approximately estimated by the proposed formulae for current RC shear walls. Therefore, the prospect was obtained that ultrahigh strength materials are applicable to RC shear walls of reactor buildings.

REFERENCES

Kodama,J. et al. (1987). Allowable Limit of Shear Walls of Reactor Buildings (Part 2) Preliminary Calculation of Limit Value, Proc. of Annual Meeting of AIJ, NO.2091.

Inoue,N. and Suzuki N. (1989). Rod Element Model for Analyzing Displacement of Reinforced Concrete Shear Walls, Analytical Studies on Shear Design of Reinforced concrete structured of JCI Colloquium.

Shiraishi,I. and Kanoh Y. (1989). Analytical study on Load-Deflection Relationship of Reinforced Concrete Shear Walls, Analytical Studies on Shear Design of Reinforced concrete structured of JCI Colloquium.

Furukawa,S. et al. (1987). Evaluation Method for Restoring Force Characteristics of R/C Shear walls of Reactor Buildings (Part 1) Evaluation Method for Restoring Force Characteristics, Proc. of Annual Meeting of AIJ, NO.2145.